

---

# Elastomers and Their Potential as Matrices in Polymer Electrolytes

---

Li Na Sim and Abdul Kariem Arof

Additional information is available at the end of the chapter

<http://dx.doi.org/10.5772/intechopen.69068>

---

## Abstract

Elastomers refer to natural or synthetic amorphous polymers which exhibit elastic properties of rubber. Elastomers are able to deform under stress and return to its original state upon removal of stress. As elastomers exhibit glass transition temperatures ( $T_g$ ) below room temperature (r.t.), elastomers are soft and rubbery at r.t, and segmental motion exists. Elastomers, which contain polar atoms, such as oxygen (O), fluorine (F) and nitrogen (N), can be suitably employed as matrices in polymer electrolytes (PEs). The electronegative atoms serve as electron donors and are able to coordinate with cations from inorganic salts to form a complex. Among elastomers that have been employed in PEs include modified and copolymerised polyisoprene or natural rubber, polyurethanes, and polysiloxanes. This chapter focuses on the progress of natural rubber and its derivatives in the field of polymer electrolytes, and discusses their interactions with other components of the PEs and ion conduction. Area percentage of ionic species, as well as ion transport parameters, such as number density, mobility and diffusion coefficient of lithium ions as obtained from deconvolution of infrared (IR) spectra, are also discussed in this book chapter.

**Keywords:** elastomers, polymer electrolytes, natural rubber, ion transport

---

## 1. Introduction

Polymer electrolytes (PEs) are ionic conductors, which consist of inorganic salts dissolved in polymer(s). Since the discovery of PEs by Fenton et al. [1], PEs are widely investigated by researchers with the aim to design flexible, light-weight, and safer solid-state ionic conductors as alternatives to the commercial leakage-prone liquid electrolytes. Excellent performing polymer electrolytes are aimed to be employed in electrochemical devices, such as fuel cells,

rechargeable batteries, solar cells, sensors, supercapacitors, and electrochromic devices. The main components of a basic PE system include a polymer matrix, which serves as medium to hold the conducting ions; an inorganic salt, which acts as source of ions or charge carriers; and a solvent, which helps to dissolve the polymer and dissociate the ions from the salt. It is widely known that ion conduction occurs predominantly in the amorphous regions of the polymer electrolyte [2]. Hence, elastomers are suitable media for ion conduction to occur as their low glass transition temperature ( $T_g$ ) below room temperature will allow high degree of polymer segmental motion to aid ion transport in polymer electrolytes.

Apart from possessing polar electron donating atoms, an elastomer has to meet certain criteria for it to be suitable for use as a polymer matrix in PEs. The elastomer also has to exhibit desirable mechanical and thermal properties, which enables it to be applicable in electrochemical devices. Complexation of cations to the polymer matrices is labile to allow ions to be transported via ion hopping and polymer segmental motion. Elastomers that have been used as polymer matrix in PEs are modified and copolymerised polyisoprene or natural rubber, polyurethanes, and polysiloxanes, which will be described briefly below. The chemical structures of natural rubber, polyurethane, and polysiloxane are depicted in **Figure 1**.

Natural rubber is widely used in many applications due to its characteristics such as flexibility, high tensile strength, being waterproof, and its availability from the rubber tree. Among applications that utilise natural rubber include tyres for vehicles, gloves and other industrial, consumer, and medical products. One of the reasons that sets natural rubber apart from the other elastomers as a preferred polymer matrix in polymer electrolytes mentioned in this chapter is that it is a natural or biopolymer, hence its sustainability and lower cost.

One setback of natural rubber is that it does not contain polar atoms that can complex with cations from salt. Hence, researchers have carried out modifications such as grafting and epoxidation to incorporate polymers possessing polar groups to allow ion transport. The use of natural rubber ( $T_g \approx -70^\circ$ ) in polymer electrolytes involves various kinds of chemical modification, that is, epoxidation and grafting, in order to introduce polar atoms into the polymer. Among all natural rubber-based polymer electrolytes, epoxidized natural rubber (ENR) (e.g. ENR-25, ENR-50; the number indicates the mole % of epoxidized group) and poly(methyl methacrylate) (PMMA)-grafted natural rubber (MG, e.g. MG30, MG45; the number indicates the percentage of PMMA-grafted) have been extensively studied [3–5]. The O atom of the epoxide group in ENR, and the carbonyl (C=O) and methoxy (C–O–CH<sub>3</sub>) groups in PMMA-grafted natural rubber are able to complex with the cations, for example, Li<sup>+</sup> or H<sup>+</sup> ions, from inorganic salts to produce ion conduction. The soft and good elastic characteristics of natural rubber also help to produce good electrode-electrolyte contact.

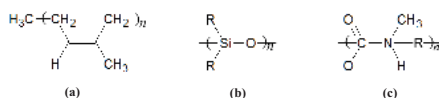


**Figure 1.** Chemical structure of (a) natural rubber, (b) polyurethane and (c) polysiloxane, where R represents an alkyl or aryl group.

Polyurethane is known for its high tensile strength and elasticity, which can be found in gaskets, cushioning, wheels and tyres for roller coasters and escalators, hoses, surface coatings and sealants, and biomedical devices. The uniqueness of polyurethane is found in its structure which is made up of alternating soft segments and hard segments connected by urethane linkages (NH—C=O—O). The soft segment of polyurethane is made up of long, flexible chains contributed by polyols, while the hard segment is made up of hydrogen bonded C=O and N—H groups contributed by isocyanates to form rigid physically cross-linked domains distributed in the soft segment matrix. In short, the soft segment provides medium for ion conduction, while the hard segment acts as reinforcing filler to provide dimensional stability. The O atoms in the soft segment of the polymer can coordinate with cations from salt to produce ion conduction. Its good adhesive property also allows good electrolyte-electrode contact during electrochemical device fabrication. Polyurethane-based polymer electrolytes have been reported to exhibit conductivity ( $\sigma$ ) around  $10^{-5}$  S cm<sup>-1</sup>. Various modified and polymer blends of polyurethane have been reported, such as cross-linked poly(urethane acrylate) [6], as well as polyurethane blended with poly(vinylidene fluoride) (PVdF) [7], poly(vinylidene fluoride-co-hexafluoropropylene) (PVdF-HFP) [8], poly(ethylene oxide) (PEO) [9, 10], and polyacrylonitrile (PAN) [11].

Another elastomer that has been employed as polymer, matrix is polysiloxane, also known as silicones. Polysiloxanes are commonly found in silicone oil, grease, rubber, resin, plastics, and so on. Polysiloxanes are inorganic comb polymers, which are composed of substituents connected to the silicon with alternating silicon and oxygen atoms. This group of polymer is known to exhibit very low  $T_g$  ( $-127^\circ\text{C}$  for poly(dimethylsiloxane)) [12], highly flexible backbone, chemical inertness, good thermal stability, and low toxicity. Due to their very low  $T_g$ , polysiloxanes exhibit low mechanical strength, and often exist as liquids or gums at room temperature. In order to impart mechanical strength into polysiloxanes, they are often cross-linked or combined with other polymers to design hybrid organic-inorganic polysiloxane-based electrolytes with good ion transport and mechanical stability. Polysiloxanes have been reported to be cross-linked with oligo(ethylene oxide) [13], oligo(ethylene glycol) [14], oligo(ethylene oxide)-co-acrylate [15], and propyl(triethylene oxide) [16], and these ether-modified polysiloxanes are seen as alternatives to poly(ethylene oxide) (PEO). Other modifications include blending of ether-modified polysiloxanes with PVdF-HFP [16, 17], and grafting of polysiloxanes with tyrenesulfonyl(phenylsulfonyl)imide [18].

In this chapter, we focus on natural rubber-based polymer matrices, that is, modified natural rubber, namely PMMA-grafted natural rubber (MG) in polymer electrolytes. The conductivity, interactions between components, crystallinity as well as glass transition temperature of MG-based polymer electrolytes containing inorganic salt, plasticizer, and filler are discussed.

## 2. PMMA-grafted natural rubber (MG)

PMMA is a promising candidate as a polymer matrix which has been widely studied in polymer electrolytes since 1985 [19]. Advantages of PMMA include its high stability towards lithium electrode, which translates to higher life cycle in lithium batteries. Being an amorphous

polymer, PMMA contains oxygen atoms in the carbonyl (C=O) and (C—O—C) groups, which can act as electron donor to complex with cations from salt. The presence of polar groups in PMMA in addition to its amorphous nature, high transparency, weatherability and good dimensional stability makes it suitable to be grafted with natural rubber. However, PMMA suffer from limitations in terms of mechanical strength and tends to be brittle [20]. Hence, combining the conducting ability of PMMA and the elasticity of natural rubber would counteract the limitations of the two polymers. The ability of PMMA to transport ions along its polymer chains combined with the resilience and flexibility of natural rubber allows PMMA-grafted natural rubber (MG), such as MG30 and MG49, to be employed as polymer matrices for ionic conductors. **Figure 2** illustrates the chemical structure of MG polymer matrix.

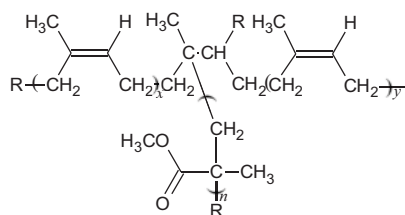


**Figure 2.** Chemical structure of MG polymer matrix. MG30 contains 30% of PMMA grafted onto natural rubber, whereas MG49 contains 49% of PMMA.

The chemical structure of MG30 and MG49 are similar and differs in the composition of PMMA which is grafted on natural rubber, where 30 and 49 represent the percentage of the methacrylate polymer present. Research on MG49 as a polymer matrix in polymer electrolytes has received more attention as compared to MG30, probably due to the higher amount of PMMA, and hence, more electron donors in the former are available for complexation with cations from salt.

### 2.1. MG-based polymer electrolytes incorporated with inorganic salts

MG-based PEs are easily prepared into films by dissolving MG polymer matrices in either toluene [21, 22] or tetrahydrofuran [5, 23] together with inorganic salt(s), and then solution casted to dry. In order to ease dissolution, the MG polymers are usually sliced into smaller pieces prior to use.

The ambient ionic conductivity of MG30 without addition of salt was reported to be in the order between  $10^{-11}$  and  $10^{-10}$  S cm<sup>-1</sup> [5, 23], which is comparable to that of other synthetic polymers. Examples of salts added into MG30 and/or MG49 are lithium triflate (LiCF<sub>3</sub>SO<sub>3</sub>) [4, 5], lithium perchlorate (LiClO<sub>4</sub>) [3], lithium tetrafluoroborate (LiBF<sub>4</sub>) [24], and ammonium triflate (NH<sub>4</sub>CF<sub>3</sub>SO<sub>3</sub>) [25], which provide ions for conduction to occur in the polymer matrix system.

Upon the incorporation of salt in MG polymer matrices, maximum conductivity is usually achieved with salt contents in the range of 15–35 wt.%. The increase in conductivity before the maximum point has been attributed to the increase in free ions [5] resulting from the

salt dissociation. This is achieved by the complexation of salt cation with the electron donor atoms in the polymer matrix or solvent, while the separated anions will move freely around in the polymer. With increasing salt content, the amount of available complexation sites on the polymer matrices will be saturated, and hence, the cations will tend to associate with anions of salt to form less mobile ion pairs or ion aggregates [5, 23]. The reduction in free ions in combination with other factors, such as lower ion mobility and increased viscosity, can be used to explain the drop in the ionic conductivity beyond the maximum point [23].

Yap et al. [5] reported the best room temperature conductivity of  $1.7 \mu\text{S cm}^{-1}$  obtained in MG30 sample containing 30 wt.%  $\text{LiCF}_3\text{SO}_3$ . The ion mechanism was found to obey the Arrhenius law, which suggested that ion transport occurs predominantly through ion hopping. The conductivity trend is in agreement with the trends of activation energy ( $E_a$ ) and amounts of free ions, whereby the best conducting sample required the lowest  $E_a$  of 0.24 eV to hop from one complexation site to another and exhibits the highest amount of free ions.

The conductivity values of MG30- and MG49-based polymer electrolytes are listed in **Table 1**. Most MG-salt complexes reported an ambient ionic conductivity around  $10^{-8}$  to  $10^{-7} \text{ S cm}^{-1}$ , which is considered insufficient for application in electrochemical devices.

Composition (wt.%)	Ambient conductivity, $\sigma$ ( $\text{S cm}^{-1}$ )	Reference
MG30: $\text{LiCF}_3\text{SO}_3$ (70:30)	$1.7 \times 10^{-6}$	[5]
MG30: $\text{LiCF}_3\text{SO}_3$ (65:35)	$8.4 \times 10^{-4}$	[4]
MG30: $\text{LiCF}_3\text{SO}_3$ :EC (15:9:76)	$9.0 \times 10^{-3}$	[4]
MG30: $\text{LiCF}_3\text{SO}_3$ :PC (26:14:60)	$3.1 \times 10^{-3}$	[23]
MG30: $\text{LiCF}_3\text{SO}_3$ :PEG200 (63:27:10)	$3.7 \times 10^{-4}$	[29]
MG30: $\text{NH}_4\text{CF}_3\text{SO}_3$ (65:35)	$2.0 \times 10^{-4}$	[25]
MG30: $\text{NH}_4\text{CF}_3\text{SO}_3$ :EC (32.5:17.5:50)	$8.9 \times 10^{-4}$	[25]
MG30: $\text{LiCF}_3\text{SO}_3$ : $\text{SiO}_2$ (60:33:7)	$\approx 2.3 \times 10^{-4}$	[28]
MG30: $\text{LiCF}_3\text{SO}_3$ : $\text{SiO}_2$ :DMC (18:9.9:2.1:70)	$\approx 3.5 \times 10^{-4}$	[28]
MG30: $\text{LiCF}_3\text{SO}_3$ : $\text{Al}_2\text{O}_3$ (59.8:32.2:8)	$1.1 \times 10^{-6}$	[31]
MG49: $\text{LiBF}_4$ (80:20)	$2.3 \times 10^{-7}$	[35, 36]
MG49: $\text{LiClO}_4$ (85:15)	$4.0 \times 10^{-8}$	[35]
MG49: $\text{LiClO}_4$ : $\text{TiO}_2$ (72:18:10)	$3.5 \times 10^{-6}$	[27]
MG49: $\text{LiClO}_4$ : $\text{TiO}_2$ :EC (49:14:7:30)	$1.1 \times 10^{-3}$	[27]
MG49: $\text{NH}_4\text{CF}_3\text{SO}_3$ -PC (3:97)	$1.2 \times 10^{-2}$	[30]
MG49: $\text{NH}_4\text{CF}_3\text{SO}_3$ -PC: $\text{SiO}_2$ (2.8:89.2:8.0)	$7.6 \times 10^{-3}$	[30]
MG49: $\text{LiClO}_4$ : [ $\text{HNO}_3$ -THF- $\text{TiO}_2$ - $\text{SiO}_2$ ] (69:23:8)	$5.86 \times 10^{-7}$	[3]

<sup>a</sup>At 30°C.

**Table 1.** Ionic conductivity values of MG-based polymer electrolytes incorporated with salt, plasticizer and filler.

## 2.2. MG-based polymer electrolytes incorporated with plasticizers

Plasticization is a common method used by researchers to enhance the ionic conductivity of polymer electrolytes. This is because plasticizers can increase the amorphousness of the polymer, and enhance polymer segmental motion and ion mobility [25]. The high dielectric constant of plasticizers can also help to dissociate the salt into free ions and prevent ion association [23]. Overall, plasticizer addition helps to improve the ionic conductivity of polymer electrolytes, which is an important factor that influences the device performance.

As mentioned earlier, most MG-based solid polymer electrolytes suffer from low conductivity ( $\sigma = 10^{-8}$  to  $10^{-7}$  S cm<sup>-1</sup>). Hence, researchers have incorporated plasticizers into MG30 and MG49 to enhance ionic conductivity. Plasticizers such as ethylene carbonate (EC) [4, 20, 21, 25–27], propylene carbonate (PC) [23], dimethyl carbonate (DMC) [28], and poly(ethylene glycol) with molecular weight of 200 (PEG200) [29] have been introduced into MG polymer matrices. **Figure 3** illustrates some examples of plasticizers that have been added into MG polymer matrices.

One of the pioneering works on MG-based polymer electrolytes is by Kumutha et al. [21] who investigated on MG30-LiCF<sub>3</sub>SO<sub>3</sub>-EC-Al<sub>2</sub>SiO<sub>5</sub> system. Results from infrared (IR) and differential scanning calorimetry (DSC) studies showed no distinct change in their wavenumbers and  $T_g$  value (which lie in the range of -39 to -42°C) upon addition of EC as plasticizer or Al<sub>2</sub>SiO<sub>5</sub> as filler. The authors reported that there is no interaction between EC, and Al<sub>2</sub>SiO<sub>5</sub>, and the polymer.

In separate works, Ali and co-workers [4, 23] investigated on MG30-LiCF<sub>3</sub>SO<sub>3</sub>-EC and MG30-LiCF<sub>3</sub>SO<sub>3</sub>-PC systems. The ionic conductivity increased from  $8.4 \times 10^{-4}$  S cm<sup>-1</sup> to achieve maximum conductivity at  $9.0 \times 10^{-3}$  S cm<sup>-1</sup> for the EC system, and  $3.1 \times 10^{-3}$  S cm<sup>-1</sup> for the system with PC on incorporation of 76 wt.% EC and 61 wt.% PC. For the MG30-LiCF<sub>3</sub>SO<sub>3</sub>-PC system, Ali et al. [23] reported that the sample containing 61 wt.% PC lost its dimensional stability despite exhibiting the best conductivity in the polymer electrolyte system. Increase in conductivity is attributed to several factors, namely increased polymer-cation interaction, high dielectric constant ( $\epsilon$ ) of EC at 89.6 (at 40°C) and PC at 64.4, which help to lower transient cross-linking between Li<sup>+</sup> ions and MG30, increased ion mobility and reduced intermolecular forces in MG30, that increased the amorphousness of the polymer in the presence of the plasticizer. The latter is manifested in the lowering of the  $T_g$  value of MG30-LiCF<sub>3</sub>SO<sub>3</sub> (65:35)

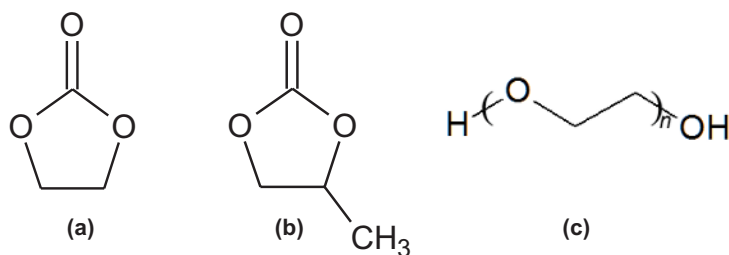


**Figure 3.** Chemical structure of (a) EC, (b) PC and (c) PEG200.

initially found between  $-66.6$  and  $-59.5^\circ\text{C}$ , and  $-77.1$  and  $-74.6^\circ\text{C}$  when 76 wt.% EC and 61 wt. of PC were added. In another work [26], gel polymer electrolytes consisting of MG30- $\text{LiCF}_3\text{SO}_3$  plasticized with 76 wt.% EC and PC were reported to exhibit lithium transference number ( $t_{\text{Li}^+}$ ) below 0.3 and voltage breakdown at 4.2 V.

Zaki et al. [25] achieved considerably high ionic conductivity of  $2.0 \times 10^{-4} \text{ S cm}^{-1}$  for MG30- $\text{NH}_4\text{LiCF}_3\text{SO}_3$  (65:35) sample. Ionic conductivity increased to  $8.9 \times 10^{-4} \text{ S cm}^{-1}$  upon introduction of 50 wt.% EC. The authors attributed the conductivity enhancement to the high dielectric constant of EC, which helped to dissociate the salt and prevent ion association. Ion conduction was found to follow Vogel-Tammann-Fulcher (VTF) behaviour, whereby ion transport occurs in the amorphous phase via polymer segmental motion. Results from XRD showed reduction in crystallinity from the gradual broadening of amorphous hump located from  $2\theta = 12^\circ$  to  $22^\circ$  with addition of EC.

In the work of Yap et al. [29], PEG was added into MG30- $\text{LiCF}_3\text{SO}_3$  system. Conductivity improved from  $1.7 \times 10^{-6} \text{ S cm}^{-1}$  to a maximum value at  $3.7 \times 10^{-4} \text{ S cm}^{-1}$ , and this was exhibited in the sample containing 10 wt.% PEG. X-ray diffraction (XRD) analysis confirmed the sample to exhibit the lowest degree of crystallinity.

### 2.3. MG-based polymer electrolytes incorporated with fillers and other additives

Although polymer electrolytes added with plasticizer exhibit conductivity enhancement, they suffer from low mechanical stability [30]. Hence, researchers have attempted using inorganic fillers to improve the physical and mechanical properties of polymer electrolytes. For MG-based polymer electrolytes, fillers that have been reported are aluminium silicate ( $\text{Al}_2\text{SiO}_5$ ) [20], silica ( $\text{SiO}_2$ ) [28, 30], alumina ( $\text{Al}_2\text{O}_3$ ) [31] and titania-silica ( $\text{TiO}_2\text{-SiO}_2$ ) [3], which are all passive fillers, and therefore do not participate directly in the  $\text{Li}^+$  ion transport process. Filler-added polymer electrolytes are known as composite polymer electrolytes (CPEs).

In the work of Hashim et al. [28],  $\text{SiO}_2$  filler was incorporated into MG30- $\text{LiCF}_3\text{SO}_3$ , followed by the addition of dimethyl carbonate (DMC) plasticizer. The ionic conductivity initially increased from  $\approx 6.0 \times 10^{-5} \text{ S cm}^{-1}$  to  $2.3 \times 10^{-4} \text{ S cm}^{-1}$  upon addition of 7 wt.%  $\text{SiO}_2$ . The rise in conductivity is attributed to the formation of conducting pathways for ion transport. Decreased conductivity above 7 wt.%  $\text{SiO}_2$  was caused by the blocking effect of the nanofillers. After that, the authors managed to further enhance the conductivity value to  $\approx 3.5 \times 10^{-4} \text{ S cm}^{-1}$  with addition of 7 wt.% DMC. The DMC plasticizer enhanced polymer segmental motion.

MG49- $\text{NH}_4\text{CF}_3\text{SO}_3$ -PC- $\text{SiO}_2$  CPE system was reported by Kamisan et al. [30]. The authors first determined the best conducting  $\text{NH}_4\text{CF}_3\text{SO}_3$  molarity in PC at 0.7 M. Gel polymer electrolyte containing 3 wt.% MG49 in the  $\text{NH}_4\text{CF}_3\text{SO}_3$ -PC liquid electrolyte exhibited high conductivity in the order of  $10^{-2} \text{ S cm}^{-1}$ . However, they lacked mechanical stability due to the high amount of liquid electrolyte. The addition of  $\text{SiO}_2$  initially decreased the conductivity to  $10^{-3} \text{ S cm}^{-1}$ , but increased to achieve two maxima at  $1.2 \times 10^{-2} \text{ S cm}^{-1}$  (3 wt.%  $\text{SiO}_2$ ) and  $7.6 \times 10^{-3} \text{ S cm}^{-1}$  (8 wt.%  $\text{SiO}_2$ ). The activation energy values calculated from the Arrhenius equation displayed two minima at 0.11 and 0.12 eV for samples with 3 and 8 wt.%  $\text{SiO}_2$  content, respectively. The CPE viscosity increased from 10.0 to 68.2 cP upon addition of 8 wt.%  $\text{SiO}_2$ , which authors took as indication of increased mechanical stability.



Kang and co-workers [3] incorporated fixed amount of  $\text{TiO}_2$ - $\text{SiO}_2$  filler into MG49- $\text{LiClO}_4$  system containing different solvents, that is,  $\text{HNO}_3$ -THF and  $\text{ClHNO}_2$ -THF. The conductivities of both MG49- $\text{LiClO}_4$ - $\text{HNO}_3$ -THF- $\text{TiO}_2$ - $\text{SiO}_2$  and MG49- $\text{LiClO}_4$ - $\text{ClHNO}_2$ -THF- $\text{TiO}_2$ - $\text{SiO}_2$  systems increased from  $1.2 \times 10^{-4} \text{ S cm}^{-1}$  to achieve a maximum at  $5.9 \times 10^{-7} \text{ S cm}^{-1}$  and  $4.8 \times 10^{-7} \text{ S cm}^{-1}$ , respectively, upon incorporation of 25 wt.%  $\text{LiClO}_4$ , before decreasing at higher salt contents. Above 25 wt.%  $\text{LiClO}_4$ , the ion transport process is hindered by ionic aggregation and the formation of transient cross-links. The two different polymer electrolyte systems exhibited different ion conduction behaviors: the system containing  $\text{HNO}_3$ -THF followed the Arrhenius rule, whereby ion transport occurs by ion hopping, whereas the  $\text{ClHNO}_2$ -THF system obeyed VTF rule, which indicates polymer segmental relaxation. Both polymer electrolyte systems are thermally stable up to around 270–290°C.

Thermal oxidation of MG-based electrolytes has also been a subject of study. Aging of polymers, which in this case is natural rubber, is a topic of concern as the unsaturated hydrocarbons will degrade on exposure to oxygen and elevated temperatures. Consequently, the physical, electrical, mechanical, and other characteristics of PEs will deteriorate upon aging. Aziz and Ali [32] studied the effect of varied contents of an antioxidant, N-(1,3-dimethylbutyl)-N'-phenyl-p-phenylenediamine (6PPD) on the thermal oxidation resistance of MG30. Using IR analysis, the absorbance/intensity ratio of the C=O band at  $1726 \text{ cm}^{-1}$  to the =C-H band located at  $\approx 835 \text{ cm}^{-1}$  of different MG30-6PPD samples were calculated to determine the degree of oxidation [33, 34]. Only the sample with 0.5 wt.% 6PPD displayed anti-oxidation effects as the intensity ratio of the bands  $1726 \text{ cm}^{-1}$ : $835 \text{ cm}^{-1}$  decreased. At higher contents of 6PPD (1, 2, 4, 6 and 8 wt.%), no anti-oxidation effect was observed. However, the MG30 sample containing 0.5 wt.% 6PPD with the best anti-oxidation effect exhibited a lower ambient conductivity of  $5.50 \times 10^{-6} \text{ S cm}^{-1}$  than the untreated sample which had conductivity of  $3.10 \times 10^{-5} \text{ S cm}^{-1}$ . The authors suggested incorporating plasticizer to increase the conductivity of MG30-6PPD sample in the future.

#### 2.4. Blends of PMMA-grafted natural rubber

In order to improve the properties of MG30- and MG49-based polymer electrolytes, researchers have attempted blending of the MG polymer matrices with other polymers. MG polymer matrices were simply mixed together with another polymer to produce polymer blend(s) which possess properties that are superior than individual polymers. MG49 has been blended with PMMA [24], PEO [36], PVdF-HFP [37], and PVdF [38]. The chemical structures of PMMA, PEO, PVdF-HFP, and PVdF are shown in **Figure 4**.

Ahmad et al. [36] found improvement in the conductivity of MG49 with and without  $\text{LiBF}_4$  salt upon blending of the polymer with 50 wt.% PMMA. Pure MG49 exhibited ambient conductivity of  $1.0 \times 10^{-12} \text{ S cm}^{-1}$ , whereas pure MG49-PMMA blend possessed conductivity of  $1.7 \times 10^{-12} \text{ S cm}^{-1}$ . Upon incorporation of  $\text{LiBF}_4$ , MG49- $\text{LiBF}_4$  and MG49-PMMA- $\text{LiBF}_4$  samples exhibited maximum conductivity of  $2.3 \times 10^{-7} \text{ S cm}^{-1}$  (at 20 wt.%) and  $8.3 \times 10^{-6} \text{ S cm}^{-1}$  (at 25 wt.%), respectively. The more superior conductivity in the polymer blend electrolyte is attributed to the higher ratio of number of oxygen atoms to lithium ion [O:Li<sup>+</sup>] of 5:1 as compared to 8:1 in single polymer electrolyte system. Morphology study by scanning electron microscopy (SEM) revealed homogenous surface in MG49 and MG49-PMMA films with no



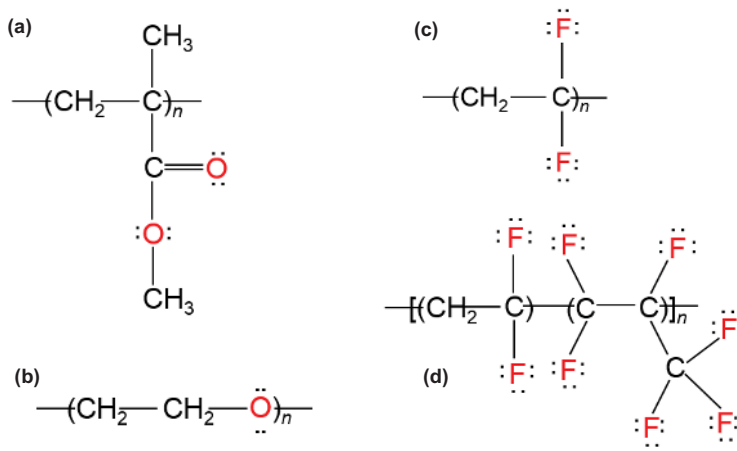


**Figure 4.** Chemical structure of (a) PMMA, (b) PEO, (c) PVdF, and (d) PVdF-HFP, where each atom in red can act as electron donor, and the black dots represent lone electrons. The polymers have been reported to be blended with MG polymer matrices.

phase separation. The changes in the structure of MG49 upon blending with PMMA indicated that intermolecular interactions between the two polymers have occurred. Crystals of  $\text{LiBF}_4$  in MG49 sample added with 25 wt.% of the salt were reported due to salt aggregation above its optimum concentration, which explained the drop in conductivity above 20 wt.%  $\text{LiBF}_4$ .

A polymer blend system that comprised PEO-MG49 with varied wt.% PEO was reported by [39]. Photograph of the PEO:MG49 with wt.% ratio of 60:40 showed a more homogeneous surface and free-standing film, as compared to other wt. ratios (80:20, 20:80, 40:60) which were not homogeneous. From SEM analyses, MG49 film was smooth due to its amorphous characteristic, while PEO film displayed rough surface attributable to its crystalline nature. Upon blending between the two polymers, homogeneous surface was reported for PEO-MG49 sample, whereby the two polymers were well distributed. With increasing addition of  $\text{LiClO}_4$ , the co-continuous phase appeared smoother and increased in pore size. Addition of PEO into MG49 was reported to improve the conductivity by two orders of magnitude. The PEO-MG49- $\text{LiClO}_4$  samples exhibited conductivity that was also higher than PEO- $\text{LiClO}_4$  sample ( $\sigma = 10^{-8}$  to  $10^{-7}$  S  $\text{cm}^{-1}$ ) [40, 41]. Maximum conductivity of  $8.0 \times 10^{-6}$  S  $\text{cm}^{-1}$  was obtained in the polymer blend incorporated with 15 wt.%  $\text{LiClO}_4$ , which was three orders higher than the sample before addition of salt ( $\sigma = 4.0 \times 10^{-9}$  S  $\text{cm}^{-1}$ ). The conductivity values of MG-based blend polymer electrolytes are listed in **Table 2**.

Su'ait and co-workers [24] blended MG49 with PMMA in the wt.% ratio of 70 to 30, and incorporated the polymer matrix with different lithium salts, namely  $\text{LiClO}_4$  and  $\text{LiBF}_4$ . The best conductivity was obtained upon addition of 25 wt.% salt in both PE systems. The PE containing  $\text{LiBF}_4$  exhibited higher conductivity ( $\sigma = 8.6 \times 10^{-6}$  S  $\text{cm}^{-1}$ ) than that of  $\text{LiClO}_4$  ( $\sigma = 1.5 \times 10^{-8}$  S  $\text{cm}^{-1}$ ) and is attributed to the larger ionic radius of  $\text{BF}_4^-$  (0.218 pm) compared to  $\text{ClO}_4^-$  (0.215 pm), and hence to the lower lattice energy of the former salt. Infrared results showed that  $\text{Li}^+$  ions complexed with the oxygen atoms present in both MG49 and PMMA.

Polymer electrolyte composition (wt.%)	Ambient conductivity (S cm <sup>-1</sup> )	Reference
MG49:PMMA (70:30)	1.1 × 10 <sup>-12</sup>	[24]
	4.1 × 10 <sup>-12</sup>	[35]
MG49:PMMA:LiClO <sub>4</sub> (52.5:22.5:25)	1.5 × 10 <sup>-8</sup>	[24]
MG49:PMMA:LiBF <sub>4</sub> (52.5:22.5:25)	8.6 × 10 <sup>-6</sup>	[24]
PEO:MG49 (60:40)	4.0 × 10 <sup>-9</sup>	[36]
PEO:MG49: LiClO <sub>4</sub> (51:34:15)	8.0 × 10 <sup>-6</sup>	[36]
PVdF-HFP: MG49: LiBF <sub>4</sub> (49:21:30)	2.8 × 10 <sup>-4</sup>	[37]
PVdF-MG49:LiTfSO <sub>3</sub> (70:30)	3.3 × 10 <sup>-4</sup>	[38]

**Table 2.** Ionic conductivity values of MG-based polymer blend electrolytes.

Among the polymer-blend electrolyte systems listed in **Table 2**, fluorine (F)-containing polymer electrolyte systems such as PVdF-HFP-MG49 [37] and PVdF-MG49 [38] achieved the best ionic conductivity up to the order of 10<sup>-4</sup> S cm<sup>-1</sup> when blended with LiBF<sub>4</sub> and LiCF<sub>3</sub>SO<sub>3</sub>, respectively. The polymer blend made up of PEO-MG49 reached the maximum conductivity from 4.0 × 10<sup>-9</sup> S cm<sup>-1</sup> to 8.0 × 10<sup>-6</sup> S cm<sup>-1</sup> upon addition of 15 wt.% LiClO<sub>4</sub>.

## 2.5. Interactions in MG-based polymer electrolytes

It is useful for researchers to investigate whether interactions have occurred between MG polymer and the salt, as well as with other components in the polymer electrolyte system, for example, plasticizer, filler, and so on, and identify the chemical group where the interactions have taken place. Interactions between components in a polymer electrolyte system will ensure miscibility and no phase separation.

As mentioned in previous sections, natural rubber does not possess polar atoms which could complex with cations from salt. In MG30 and MG49, the PMMA contains oxygen atoms in the C=O and C—O—C groups which have been reported to interact with the cations from salt through coordination bond(s) [4, 5, 20, 23, 24]. Evidence of complexation of MG30 and MG49 with various salts could be obtained from infrared (IR) spectroscopy. The wavenumber regions of interest of MG polymer matrices are ≈1720–1750 cm<sup>-1</sup> and ≈950–1450 cm<sup>-1</sup> which represent the C=O and C—O—C group, respectively. Shifting of the IR bands mentioned indicates complexation of MG polymer with cations from the salt.

Although interactions between MG polymer matrix and salt are usually shown from the shifting of the symmetrical C=O stretching ( $\nu(\text{C}=\text{O})$ ) and IR bands corresponding to the C—O—C group of PMMA, that is, combined C—O—O stretching ( $\nu(\text{C}-\text{O}-\text{O})$ ) and C—O stretching ( $\nu(\text{C}-\text{O})$ ), symmetric, and asymmetric stretching of C—O—C group ( $\nu_s(\text{C}-\text{O}-\text{C})$  and  $\nu_{as}(\text{C}-\text{O}-\text{C})$ ) as well as deformation of O—CH<sub>3</sub> ( $\delta(\text{O}-\text{CH}_3)$ ), some researchers did not find significant wavenumber shift that is beyond the resolution used to measure the IR spectra. Su'ait and co-workers [24] investigated on MG49-PMMA blend incorporated with different lithium salts, namely LiBF<sub>4</sub> and LiClO<sub>4</sub>. The  $\nu(\text{C}=\text{O})$  band in the samples containing 10 and 20 wt.%

respective salt did not show wavenumber change but reduced in intensity. Other bands such as the combined  $\nu(\text{C—O—O})$  and  $\nu(\text{C—O})$  band at  $1272\text{ cm}^{-1}$  and  $\nu_{\text{s}}(\text{C—O—C})$  at  $985\text{ cm}^{-1}$  also did not manifest any IR wavenumber shift. The intensity of the  $\nu_{\text{as}}(\text{C—O—C})$  band was noticeably reduced upon addition of 20 wt.%  $\text{LiBF}_4$ . Only the  $\delta(\text{O—CH}_3)$  band shifted from  $1455\text{ cm}^{-1}$  to  $1460\text{ cm}^{-1}$  and  $1461\text{ cm}^{-1}$  in  $\text{LiClO}_4$  and  $\text{LiBF}_4$ -added samples, respectively. The reduction in intensity and wavenumber shifts indicated complexation has taken place between  $\text{Li}^+$  ions from the salts and MG49.

Several reports on plasticized MG-based polymer electrolytes found no interaction from IR studies between the polymer matrix and the plasticizer. Kumutha and co-workers [21] reported on the IR analyses of MG30- $\text{LiCF}_3\text{SO}_3$ -EC system and explored the interactions between MG30 and EC and between  $\text{LiCF}_3\text{SO}_3$  and EC. For the MG30-EC sample, no IR change was found, which indicated that there was no interaction between the polymer and plasticizer. However, for the  $\text{LiCF}_3\text{SO}_3$ -EC mixture, the  $\nu(\text{C=O})$ , C=O bending, and ring breathing of EC shifted from  $1803$  to  $1778\text{ cm}^{-1}$ , from  $718$  to  $720\text{ cm}^{-1}$  and from  $897$  to  $899\text{ cm}^{-1}$ , respectively, which suggested that interaction has occurred between the C=O group of EC and  $\text{Li}^+$  ions from the salt to form C=O... $\text{Li}^+$  interaction. Hence, EC has penetrated into the MG30- $\text{LiCF}_3\text{SO}_3$  complex with interaction with the salt but no interaction with the polymer.

Ali et al. [23] investigated on MG30- $\text{LiCF}_3\text{SO}_3$ -PC system. The  $\nu(\text{C=O})$  of PC displayed down-shift from  $1788$  to  $1775\text{ cm}^{-1}$  in the  $\text{LiCF}_3\text{SO}_3$ -PC mixture, which showed coordination of  $\text{Li}^+$  ions onto the C=O group of PC. Similar to [21], no IR change was observed for MG30-PC sample, which suggested no interaction between the polymer and the plasticizer.

In filler-added polymer electrolyte system, such as MG30- $\text{LiCF}_3\text{SO}_3$ -EC- $\text{Al}_2\text{SiO}_5$ , Kumutha et al. [20] did not observe any IR change to the spectra of polymer electrolyte upon incorporation of the filler. This indicates that  $\text{Al}_2\text{SiO}_5$  did not interact with the components in the PE complex and only existed as dispersed solid.

The formation of MG49-PMMA blend was investigated by Ahmad et al. [36] using IR spectroscopy. The  $\delta(\text{O—CH}_3)$  and  $\nu_{\text{s}}(\text{C—O—C})$  bands of pure MG49 shifted from  $984$  and  $1457\text{ cm}^{-1}$  to  $992$  and  $1450\text{ cm}^{-1}$  in MG49-PMMA blend, respectively, which indicated the occurrence of intermolecular interactions between MG49 and PMMA. Upon addition of  $\text{LiBF}_4$  salt, several bands of MG49 and MG49-PMMA shifted, which suggested complexation between  $\text{Li}^+$  ions and the polymer matrix. The  $\nu_{\text{s}}(\text{C—O—C})$  shifted from  $984$  to  $987\text{ cm}^{-1}$  in MG49- $\text{LiBF}_4$  sample, and from  $992$  to  $985\text{ cm}^{-1}$  in MG49-PMMA- $\text{LiBF}_4$  sample; the band reduced in intensity in both systems. The  $\delta(\text{O—CH}_3)$  also shifted from  $1450$  and  $1457\text{ cm}^{-1}$  in MG49- $\text{LiBF}_4$  and MG49-PMMA- $\text{LiBF}_4$ , respectively, to  $1461\text{ cm}^{-1}$ . From the results, the authors implied that oxygen in the C—O—C group of PMMA interacted at a higher extent to  $\text{Li}^+$  ions.

For PEO-MG49- $\text{LiClO}_4$  polymer blend electrolyte system, complexation between  $\text{Li}^+$  ions and the polymer blend was confirmed by Ahmad and co-workers [39] from the shifting of bands belonging to PEO and PMMA in MG49. The triple band due to PEO initially located at  $1146$ ,  $1099$ , and  $1060\text{ cm}^{-1}$  formed a single band in the range of  $1066$ – $1094\text{ cm}^{-1}$  in PEO-MG49- $\text{LiClO}_4$  samples, which indicated coordination of  $\text{Li}^+$  ions on the O atoms in PEO. The  $\delta(\text{O—CH}_3)$  of PMMA in MG49 also shifted from  $1466\text{ cm}^{-1}$  to lower wave numbers to around  $1450\text{ cm}^{-1}$  in the  $\text{LiClO}_4$ -containing polymer blend electrolytes.

## 2.6. Determination of free ion, ion pairs and ion aggregates

Besides being able to reveal the interactions that occur in polymer electrolyte systems, IR analysis can also estimate the amount of charge carriers present in different samples. The result can be used to explain the conductivity behavior at different added contents of salt or other additives in the polymer electrolyte system.

Some IR regions representing certain bands of the salt could reveal the types of ionic species (i.e. free ions, ion pairs, ion aggregates) present and their area percentage in the polymer electrolytes. According to Huang and Frech [42], different types of triflate ( $\text{CF}_3\text{SO}_3^-$ ) ionic species can be distinguished from the deconvolution of the IR envelope of symmetrical stretching of  $\text{SO}_3$  ( $\nu_s(\text{SO}_3)$ ) of the salt. Free ions, ion pairs and ion aggregates could be distinguished at  $1030\text{--}1034\text{ cm}^{-1}$ ,  $1040\text{--}1045\text{ cm}^{-1}$ , and  $1049\text{--}1053\text{ cm}^{-1}$ , respectively [42].

Yap et al. [5] studied MG30 PE system added with varied  $\text{LiCF}_3\text{SO}_3$  contents and noted the increase of conductivity up to 30 wt.%  $\text{LiCF}_3\text{SO}_3$  with maximum conductivity of  $1.7\ \mu\text{S cm}^{-1}$  at  $30^\circ\text{C}$  before dropping beyond that composition. The IR spectra of  $\text{LiCF}_3\text{SO}_3$ , MG30, and MG30- $\text{LiCF}_3\text{SO}_3$  samples between  $1000$  and  $1100\text{ cm}^{-1}$ , where the  $\nu_s(\text{SO}_3)$  of  $\text{LiCF}_3\text{SO}_3$  lies, are illustrated in **Figure 5**. The band observed at  $1044\text{ cm}^{-1}$  in  $\text{LiCF}_3\text{SO}_3$  sample corresponded to the ion pairs of the salt. Upon incorporation of  $\text{LiCF}_3\text{SO}_3$  into MG30, a band located at  $1032\text{ cm}^{-1}$  attributed to free ions was found in all MG30- $\text{LiCF}_3\text{SO}_3$  samples. A shoulder appeared around  $1040\text{ cm}^{-1}$  (as shown by the dotted line in **Figure 5**). In order to separate the IR envelope from  $1000$  to  $1060\text{ cm}^{-1}$  in the varied MG30- $\text{LiCF}_3\text{SO}_3$  samples, IR deconvolution was carried out as shown in **Figure 6**.

Yap and co-workers [5] reported the presence of free ions ( $1032\text{ cm}^{-1}$ ) and ion pairs ( $1040\text{ cm}^{-1}$ ) in the MG30- $\text{LiCF}_3\text{SO}_3$  samples. No ion aggregate was detected in the samples. The trend of free ions obeyed the trend of conductivity, whereby the highest area % of free ions was found in the best conducting sample, which is MG30 containing 30 wt.%  $\text{LiCF}_3\text{SO}_3$ . Increasing free ions with  $\text{LiCF}_3\text{SO}_3$  contents is due to the recombination of  $\text{Li}^+$  and  $\text{CF}_3\text{SO}_3^-$  ions. Hence, the trend of conductivity, that is, the rise of conductivity below 30 wt.%  $\text{LiCF}_3\text{SO}_3$  and its subsequent drop above that composition was explained by the trend of free ions.

## 2.7. Determination of number density, mobility and diffusion coefficient values

By using the % area of free ions obtained from the IR deconvolution of  $\nu_s(\text{SO}_3)$  band belonging to  $\text{LiCF}_3\text{SO}_3$  for MG30- $\text{LiCF}_3\text{SO}_3$  samples, ion transport parameters, such as number density ( $n$ ), mobility ( $\mu$ ), and diffusion coefficient ( $D$ ), could be calculated using the equations below:

$$n = \%FI \times \frac{m}{M_w} \times \frac{N_A}{V} \quad (1)$$

$$\mu = \frac{\sigma}{n \times e} \quad (2)$$

$$D = \frac{\mu \times k \times T}{e} \quad (3)$$

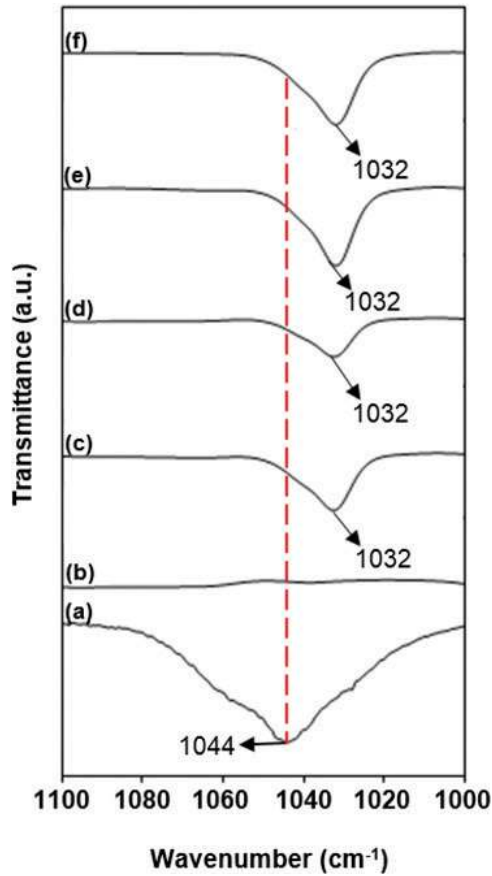


**Figure 5.** IR spectra between 1000 and 1100  $\text{cm}^{-1}$  of (a)  $\text{LiCF}_3\text{SO}_3$ , (b) MG30, (c) MG30- $\text{LiCF}_3\text{SO}_3$  (90:10), (d) MG30- $\text{LiCF}_3\text{SO}_3$  (80:20), (e) MG30- $\text{LiCF}_3\text{SO}_3$  (70:30), and (f) MG30- $\text{LiCF}_3\text{SO}_3$  (60:40).

Where %FI represents the percentage of free  $\text{Li}^+$  ions obtained from IR deconvolution,  $m$  refers to mass of  $\text{LiCF}_3\text{SO}_3$  used,  $M_w$  is the molecular mass of  $\text{LiCF}_3\text{SO}_3$  ( $156.01 \text{ g mol}^{-1}$ ),  $N_A$  Avogadro's number ( $6.02 \times 10^{23}$ ),  $V$  is the total volume of components present in the sample,  $\sigma$  is the conductivity of every sample at 298 K,  $e$  is the electron charge ( $1.60 \times 10^{-19} \text{ C}$ ),  $k$  is the Boltzmann constant ( $1.38 \times 10^{-23} \text{ J K}^{-1}$ ), and  $T$  is 298 K. The density of  $\text{LiCF}_3\text{SO}_3$  is  $1.90 \text{ g cm}^{-3}$ , while the density of MG30 (natural rubber:PMMA = 70:30) was taken to be  $1.005 \text{ g cm}^{-3}$ . The value  $n$  corresponds to the number density of mobile ions,  $\mu$  value refers to the mobility attained by the  $\text{Li}^+$  ions under application of electric field, and  $D$  value gives the rate at which  $\text{Li}^+$  ions are transported within a second. **Table 3** lists the conductivity, % area of free ions,  $n$ ,  $\mu$ , and  $D$  for MG30 added with varied wt.%  $\text{LiCF}_3\text{SO}_3$ . It was found that the  $n$  increased continuously up to 40 wt.%  $\text{LiCF}_3\text{SO}_3$ , while both  $\mu$  and  $D$  were highest at 30 wt.%  $\text{LiCF}_3\text{SO}_3$ , which indicates that the ion transport is diffusion controlled. As the MG30 added with 30 wt.%  $\text{LiCF}_3\text{SO}_3$  exhibited the best conductivity and the lowest degree of crystallinity [5],  $\text{Li}^+$  ions are more mobile and are able to diffuse more easily through the amorphous region in the sample.

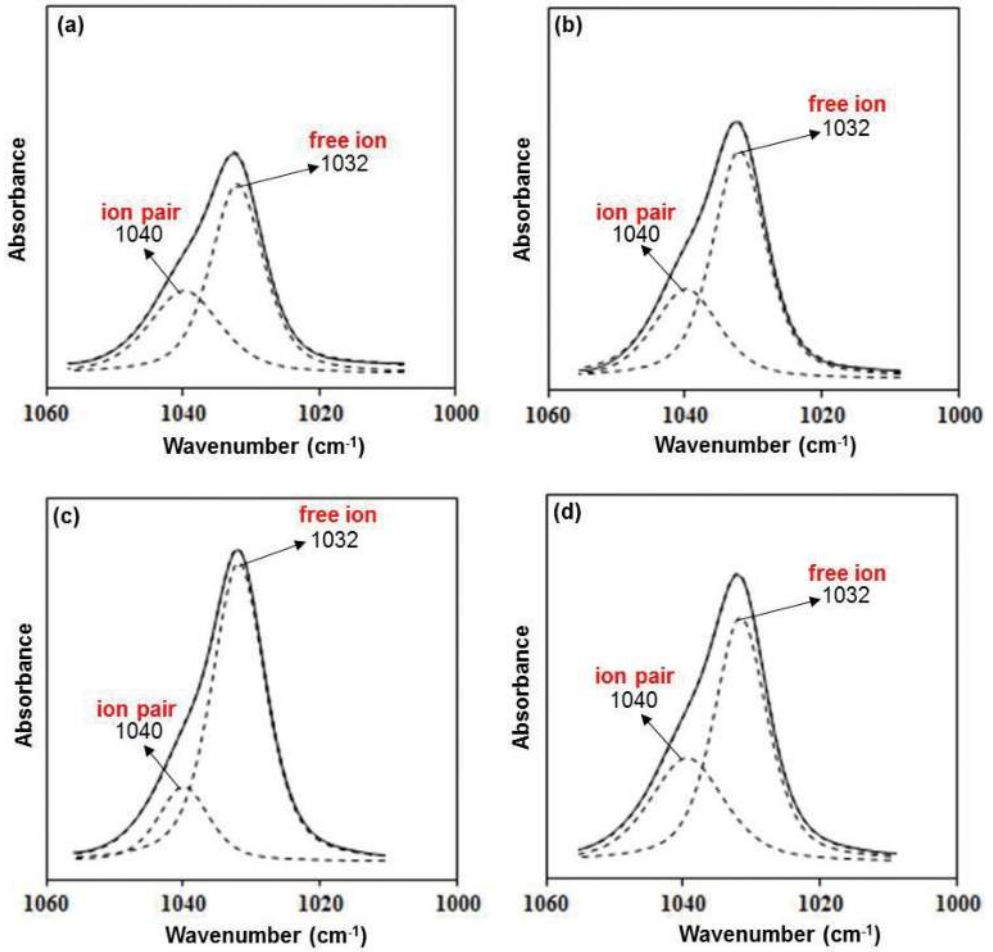


Figure 6. IR deconvolution of  $\nu_s(\text{SO}_3)$  band belonging to  $\text{LiCF}_3\text{SO}_3$  in  $\text{MG30}:\text{LiCF}_3\text{SO}_3$  system with wt.% ratio of (a) 90:10, (b) 80:20, (c) 70:30, and (d) 60:40.

$\text{LiCF}_3\text{SO}_3$ content (wt.%)	$\sigma$ ( $\text{S cm}^{-1}$ )	FI (%)	$n$ ( $\text{cm}^{-3}$ )	$\mu$ ( $\text{cm}^2\text{V}^{-1}\text{s}^{-1}$ )	$D$ ( $\text{cm}^2 \text{s}^{-1}$ )
10	$1.9 \times 10^{-9}$	67.0	$2.7 \times 10^{22}$	$4.3 \times 10^{-13}$	$1.1 \times 10^{-14}$
20	$1.1 \times 10^{-8}$	70.0	$6.0 \times 10^{22}$	$1.1 \times 10^{-12}$	$2.9 \times 10^{-14}$
30	$1.7 \times 10^{-6}$	78.2	$1.1 \times 10^{23}$	$10.0 \times 10^{-11}$	$2.6 \times 10^{-12}$
40	$6.4 \times 10^{-8}$	68.6	$1.3 \times 10^{23}$	$3.1 \times 10^{-12}$	$7.8 \times 10^{-14}$

Table 3. Conductivity ( $\sigma$ ), % area of free ions (FI), number density ( $n$ ), mobility ( $\mu$ ) and diffusion coefficient ( $D$ ) of  $\text{Li}^+$  ions of MG30 samples added with varied  $\text{LiCF}_3\text{SO}_3$  contents.

### 3. Summary

Modified natural rubbers namely PMMA-grafted natural rubber (i.e. MG30 and MG49), are widely used as polymer matrices in polymer electrolytes. MG30 and MG49 contain polar C=O and C—O—C groups which could complex with cations from salt to produce ion transport. Plasticizers, such as EC, PC, DMC, and PEG200, were employed to enhance the conductivity of solid-based MG polymer matrices. Passive inorganic fillers, such as SiO<sub>2</sub>, Al<sub>2</sub>O<sub>3</sub>, TiO<sub>2</sub>, TiO<sub>2</sub>-SiO<sub>2</sub>, were used to improve the mechanical strength of the polymer electrolytes. Polymer blends of MG with PEO, PMMA, PVdF, and PVdF-HFP were able to improve the properties of MG-based polymer electrolytes in terms of conductivity and structural homogeneity. Complexation between MG polymer matrices and salt could usually be shown through IR shifts of bands corresponding to C=O and C—O—C groups, although in some cases, only changes in intensity were reported. Plasticizers and fillers added into MG polymer matrices did not manifest change on the IR spectra of the polymer, although interactions were found to occur between plasticizer and the salt (i.e., between LiCF<sub>3</sub>SO<sub>3</sub> and EC or PC). MG30 and MG49-based polymer electrolytes could achieve high ionic conductivity up to 10<sup>-2</sup> S cm<sup>-1</sup> when plasticized and have potential to be used in electrochemical devices.

### Acknowledgements

The authors would like to thank Ministry of Higher Education (MOHE) for grant FP053-2014A, SATU Joint Research Scheme RU022G-2014 and University of Malaya.

### Author details

Li Na Sim and Abdul Kariem Arof\*

\*Address all correspondence to: [akarof@um.edu.my](mailto:akarof@um.edu.my)

Department of Physics, Faculty of Science, Centre for Ionics University Malaya, University of Malaya, Kuala Lumpur

### References

- [1] Fenton DE, Parker JM, Wright PV. Complexes of alkali metal ions with poly (ethylene oxide). *Polymer*. 1973;**14**:589
- [2] Berthier C, Gorecki W, Minier M, Armand MB, Chabagno JM, Rigaud P. Microscopic investigation of ionic conductivity in alkali metal salts–poly(ethylene oxide) adducts. *Solid State Ionics*. 1983;**11**:91-95



- [3] Kang OL, Ahmad A, Hassan NH, Rana UA. [MG49-LiClO<sub>4</sub>]:[TiO<sub>2</sub>-SiO<sub>2</sub>] polymer electrolytes: In situ preparation and characterization. *International Journal of Polymer Science*. 2016;**9838067**
- [4] Ali AMM, Subban RHY, Bahron H, Yahya MZA, Kamisan AS. Investigation on modified natural rubber gel polymer electrolytes for lithium polymer battery. *Journal of Power Sources*. 2013;**244**:636-640
- [5] Yap KS, Teo LP, Sim LN, Majid SR, Arof AK. Investigation on dielectric relaxation of PMMA-grafted natural rubber incorporated with LiCF<sub>3</sub>SO<sub>3</sub>. *Physica B*. 2012;**407**: 2421-2428
- [6] Santhosh P, Gopalan A, Vasudevan T, Lee KP. Evaluation of a cross-linked polyurethane acrylate as polymer electrolyte for lithium batteries. *Materials Research Bulletin*. 2006;**41**:1023-1037
- [7] Wu N, Cao Q, Wang X, Li S, Li X, Deng H. In situ ceramic fillers of electrospun thermoplastic polyurethane/poly(vinylidene fluoride) based gel polymer electrolytes for Li-ion batteries. *Journal of Power Sources*. 2011;**196**:9751-9756
- [8] Zhou L, Jing B, Wang X, Tang X, Wu N. Study of a novel porous gel polymer electrolyte based on thermoplastic polyurethane/poly(vinylidene fluoride-co-hexafluoropropylene) by electrospinning technique. *Journal of Power Sources*. 2014;**263**:118-124
- [9] Yoshimoto N, Nomura H, Shirai T, Ishikawa M, Morita M. Ionic conductance of gel electrolyte using a polyurethane matrix for rechargeable lithium batteries. *Electrochimica Acta*. 2004;**50**:275-279
- [10] Wen TC, Chen WC. Gelled composite electrolyte comprising thermoplastic polyurethane and poly(ethylene oxide) for lithium batteries. *Journal of Power Sources*. 2001;**92**:139-148
- [11] Wen TC, Kuo HH, Gopalan A. The influence of lithium ions on molecular interaction and conductivity of composite electrolyte consisting of TPU and PAN. *Solid State Ionics*. 2002;**147**:171-180
- [12] Song JY, Wang YY, Wan CC. Review of gel-type polymer electrolytes for lithium-ion batteries. *Journal of Power Sources*. 1999;**77**:183-197
- [13] Kang Y, Lee W, Suh DH, Lee C. Solid polymer electrolytes based on cross-linked polysiloxane-g-oligo(ethylene oxide): Ionic conductivity and electrochemical properties. *Journal of Power Sources*. 2003;**119-121**:448-453
- [14] Zhang ZC, Jin JJ, Bautista F, Lyons LJ, Shariatzadeh N, Sherlock D, Amine K, West R. Ion conductive characteristics of cross-linked network polysiloxane-based solid polymer electrolytes. *Solid State Ionics*. 2004;**170**:233-238
- [15] Kang Y, Lee J, Suh DH, Lee C. A new polysiloxane based cross-linker for solid polymer electrolyte. *Journal of Power Sources*. 2005;**146**:391-396
- [16] Cznotka E, Jeschke S, Wiemhofer H-D. Characterization of semi-interpenetrating polymer electrolytes containing poly(vinylidene fluoride-co-hexafluoropropylene) and ether-modified polysiloxane. *Solid State Ionics*. 2016;**289**:35-47

- [17] Seidel SM, Jeschke S, Vettikuzha P, Wiemhofer HD. PVDF-HFP/ether-modified polysiloxane membranes obtained via airbrush spraying as active separators for application in lithium ion batteries. *Chemical Communications*. 2015;**51**:12048-12051
- [18] Rohan R, Pareek K, Chen Z, Cai W, Zhang Y, Xu G, Gao Z, Cheng H. A high performance polysiloxane-based single ion conducting polymeric electrolyte membrane for application in lithium ion batteries. *Journal of Materials Chemistry A*. 2015;**3**:20267-20276
- [19] Iijima T, Tyoguchi Y, Eda N. Quasi-solid organic electrolytes gelatinized with PMMA and their applications for lithium batteries. 1985;**53**:619-623
- [20] Brown H. A molecular interpretation of the toughness of glassy polymers. *Macromolecules*. 1991;**24**:2752-2756
- [21] Kumutha K, Alias Y, Said R. FTIR and thermal studies of modified natural rubber based polymer electrolytes. *Ionics*. 2005;**11**:472-476
- [22] Kumutha K, Alias Y. FTIR spectra of plasticized grafted natural rubber-LiCF<sub>3</sub>SO<sub>3</sub> electrolytes. *Spectrochimica Acta Part A*. 2006;**64**:442-447
- [23] Ali AMM, Subban RHY, Bahron H, Winie T, Latif F, Yahya MZA. Grafted natural rubber-based polymer electrolytes: ATR-FTIR and conductivity studies. *Ionics*. 2008;**14**:491-500
- [24] Su'ait MS, Ahmad A, Hamzah H, Rahman MYA. Effect of lithium salt concentrations on blended 49% poly(methyl methacrylate) grafted natural rubber and poly(methyl methacrylate) based solid polymer electrolyte. *Electrochimica Acta*. 2011;**57**:123-131
- [25] Zaki NHM, Mahmud ZS, Yahya MZA, Ali AMM. Conductivity studies on 30% PMMA grafted NR-NH<sub>4</sub>CF<sub>3</sub>SO<sub>3</sub> Gel Polymer Electrolytes. 2012 IEEE Symposium on Humanities, Science and Engineering Research. 2012;**6268995**:797-800
- [26] Ali AMM, Yahya MZA, Bahron H, Subban RHY. Electrochemical studies on polymer electrolytes based on poly(methyl methacrylate)-grafted natural rubber for lithium polymer battery. *Ionics*. 2006;**12**:303-307
- [27] Low SP, Ahmad A, Rahman MYA. Effect of ethylene carbonate plasticizer and TiO<sub>2</sub> nanoparticles on 49% poly(methyl methacrylate) grafted natural rubber-based polymer electrolyte. *Ionics*. 2010;**16**:821-826
- [28] Hashim H, Adam NI, Zaki NHM, Mahmud ZS, Said CMS, Yahya MZA, Ali AMM. Natural rubber-grafted with 30% poly(methylmethacrylate) characterization for application in lithium polymer battery. 2010 International Conference on Science and Social Research. 2010;**5773825**:485-488
- [29] Yap KS, Teo LP, Sim LN, Majid SR, Arof AK. Plasticised polymer electrolytes based on PMMA grafted natural rubber-LiCF<sub>3</sub>SO<sub>3</sub>-PEG200. *Materials Research Innovations*. 2011;**15**:34-38
- [30] Kamisan AS, Kudin TIT, Ali AMM, Yahya MZA. Electrical and physical studies on 49% methyl-grafted natural rubber-based composite polymer gel electrolytes. *Electrochimica Acta*. 2011;**57**:207-211

- [31] Adam NI, Zaki NHM, Mahmud ZS, Yahya MZA. The effect of composition nanofiller Al<sub>2</sub>O<sub>3</sub> to the conductivity, morphology and thermal properties of MG30-LiTf polymer electrolyte. IEEE Symposium on Business, Engineering and Industrial Applications. 2012;**6422980**:701-704
- [32] Aziz AFB, Ali AMM. Thermal oxidation studies on methyl grafted natural rubber polymer electrolytes with paraphenylene diamine additive. 2012 IEEE Colloquium on Humanities, Science and Engineering Research. 2012;**6504406**:719-723
- [33] Li GY, Koenig JL. FTIR imaging of oxidation of polyisoprene 2. The role of N-phenyl-Ng-dimethyl-butyl-p-phenylenediamine antioxidant. Polymer Degradation and Stability. 2003;**81**:377-385
- [34] Narathichat M, Sahakaro K, Nakason C. Assessment degradation of natural rubber by moving die processability test and FTIR spectroscopy. Journal of Applied Polymer Science. 2010;**115**:1702-1709
- [35] Su'ait MS, Ahmad A, Rahman MYA. Ionic conductivity studies of 49% poly(methyl methacrylate)-grafted natural rubber-based solid polymer electrolytes. Ionics. 2009;**15**: 497-500
- [36] Ahmad A, Rahman MYA, Su'ait MS, Hamzah H. Study of MG49-PMMA based polymer electrolyte. The Open Materials Science Journal. 2011;**5**:170-177
- [37] Ataollahi N, Ahmad A, Hamzah H, Rahman MYA, Mohamed NS. Preparation and characterization of PVDF-HFP/MG49 based polymer blend electrolyte. International Journal of Electrochemical Science. 2012;**7**:6693-6703
- [38] TianKhoon L, Ataollahi N, Hassan NH, Ahmad A. Studies of porous solid polymeric electrolytes based on poly(vinylidene fluoride) and poly(methyl methacrylate) grafted natural rubber for applications in electrochemical devices. Journal of Solid State Electrochemistry. 2016;**20**:203-213
- [39] Ahmad A, Rahman MYA, Su'ait MS. Morphological, infrared, and ionic conductivity studies of poly(ethylene oxide)-49% poly(methyl methacrylate) grafted natural rubber-lithium perchlorate salt based solid polymer electrolytes. Journal of Applied Polymer Science. 2012;**124**:4222-4229
- [40] Xi J, Qiu X, Zheng S, Tang X. Nanocomposite polymer electrolyte comprising PEO/LiClO<sub>4</sub> and solid super acid: Effect of sulphated-zirconia on the crystallization kinetics of PEO. Polymer. 2005;**46**:5702-5706
- [41] Abdullah M, Lenggoro W, Okuyama. Polymer electrolyte nanocomposites. In: Nalwa HS, editor. Encyclopedia Nanoscience and Nanotechnology. American Scientific Publishers; USA: American Scientific Publishers; 2004. p. 731
- [42] Huang W, Frech R. Dependence of ionic association on polymer chain length in poly(ethylene oxide)-lithium triflate complexes. Polymer. 1994;**35**:235-242